Electronic Supplementary Information (ESI) for

Carbon coated porous titanium niobium oxides as anode materials of lithium ion batteries for extreme fast charge applications

Hailong Lyu[ab*], Jianlin Li[c], Tao Wang[b], Bishnu P Thapaliya[ab], Shuang Men[a], Charl J. Jafta[ac], Runming Tao[b], Xiao-Guang Sun[a*], and Sheng Dai[ab*]

[a] Chemical Sciences Division, Oak Ridge National Laboratory, Oak Ridge, TN 37831, USA.

[b] Department of Chemistry, University of Tennessee, Knoxville, TN 37996, USA

[c] Energy and Transportation Science Division, Oak Ridge National Laboratory, Oak Ridge, TN 37830, USA

*Corresponding authors. E-mail: lyuh@ornl.gov; sunx@ornl.gov; dais@ornl.gov

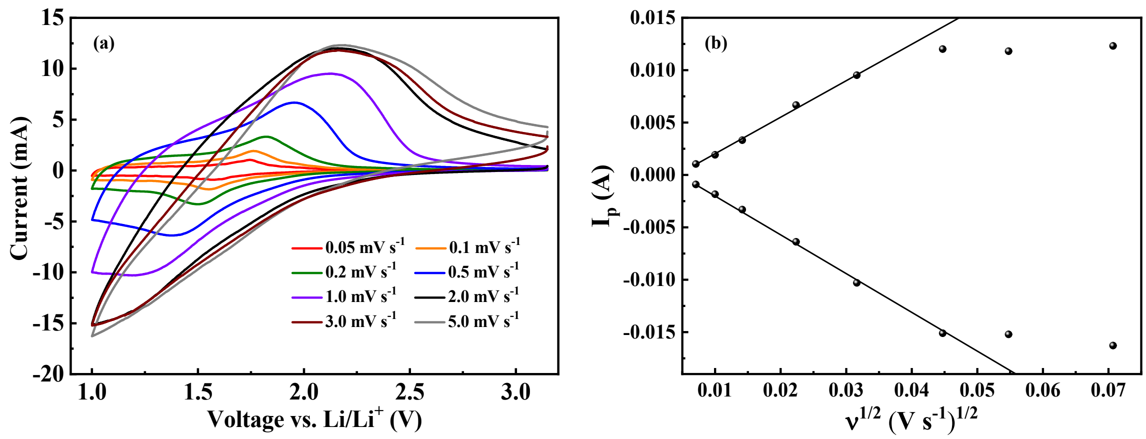

Figure S1. (a) CV profiles of TNO@C half-cell at various scan rates from 0.05 to 5.0 mV s^{-1}; (b) relationships between the peak current (I_p) and the square root of scan rate ($\nu^{1/2}$) in lithiation and delithiation processes of TNO@C half-cell.

The Li ion diffusion coefficients are calculated using the Randles–Sevcik equation (Eqn. 1):

$$I_p = 269000n^{3/2}AD^{1/2}Cv^{1/2} \tag{1}$$

In Eqn. 1, I_p is the peak current (A), n is the electrons concentration per molecule during the redox reactions, A is the surface area of the electrodes (cm^2), D is the diffusion coefficient of lithium ions (cm^2 s^{-1}), C is the bulk concentration of lithium ions in electrodes (mol cm^{-3}) and v is the scan rate (V s^{-1}). A linear relationship between I_p and $v^{1/2}$ can be found according to Eqn. 1, as well as the results displayed in Figure S1b. The diffusion coefficients of lithium ions in TNO@C are calculated through the slopes, which are estimated to be 2.39×10^{-12} and 2.13×10^{-12} cm^2 s^{-1} for lithiation and delithiation processes, respectively. Besides, the values of I_p change little above the scan rate of 2.0 mV s^{-1}, that is, about 16.67 mins scan time, suggesting the diffusion coefficient of lithium ions would be the limitation to extreme fast charging (XFC) performance of high-loading TNO@C anodes shorter than 16.67 mins.

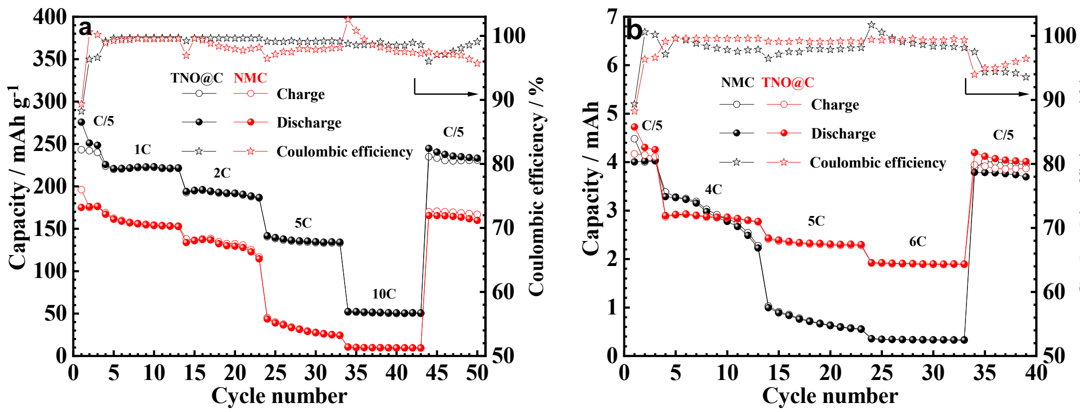

Figure S2. (a) Specific capacities and coulombic efficiencies and (b) high rate performance and coulombic efficiencies of NMC and TNO@C half-cells (18 and 13.5 mg/cm^2 for NMC622 and TNO@C, respectively).

For the NMC half-cell, the charge rates changed while the discharge rate was fixed at C/3, whereas for the TNO@C half-cell, the discharge current rates changed while the charge rate was fixed at C/3 (1C=150 mA/g for NMC622 and 200 mA/g for TNO@C).

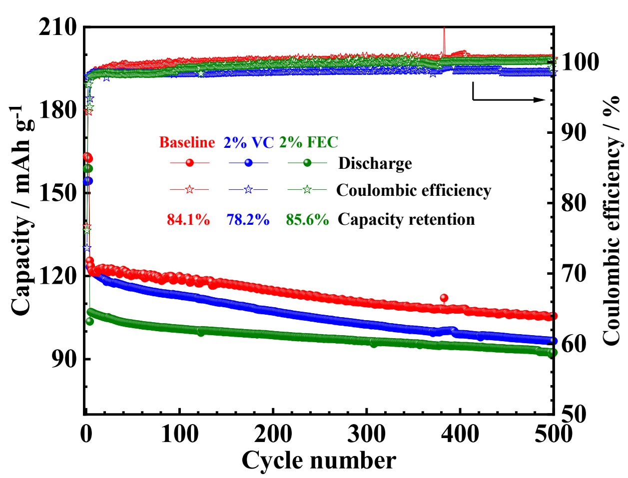

Figure S3. Cycling performance of NMC/TNO@C full-cells with different electrolytes under the 5C charging protocol.

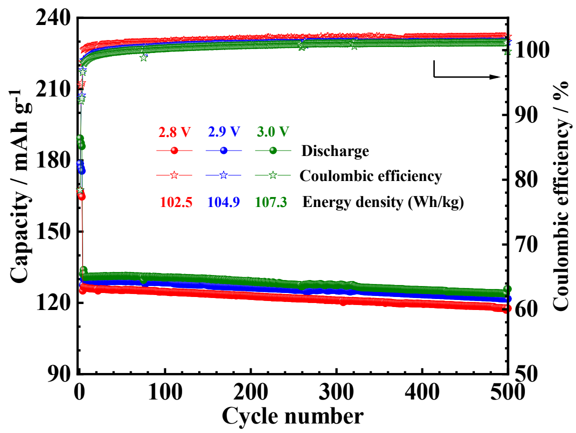

Figure S4. Cycling performance of NMC/TNO@C full-cells with different upper cut-off voltages under the 4C charging protocol.

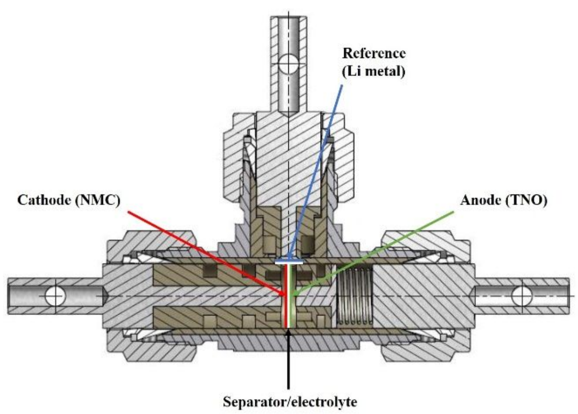

Figure S5. Schematic illustration of the three-electrode Swagelok full-cell.

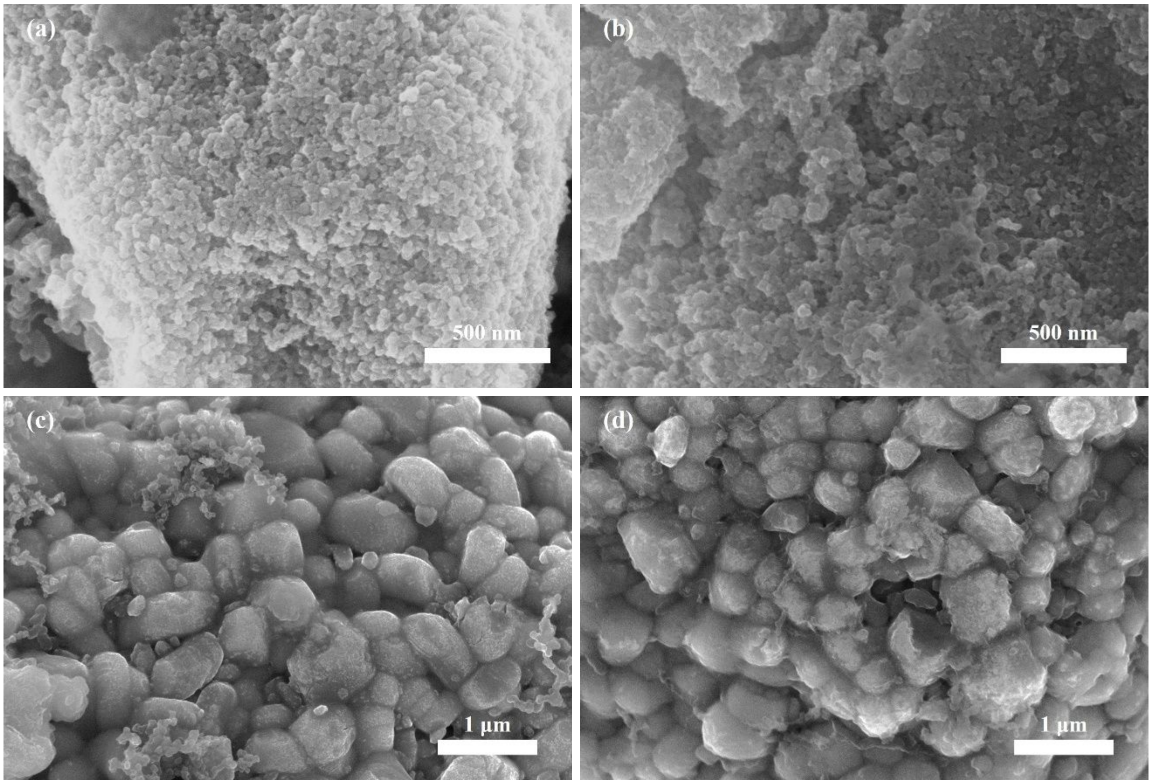

Figure S6. SEM images of (a & b) TNO@C and (c & d) NMC electrodes (a & c) before and (b & d) after XFC cycling, respectively.

Table S1. Energy density and energy retention of NMC/TNO@C full-cells with different TNO loadings.

TNO loading (mg/cm^2)	4.3	6.8	9.5	13.4
Mass energy density (Wh/kg)	105.6	106.7	114.7	102.5
Volume energy density (Wh/L)	264	267	287	256
Energy retention after 500 cycles (%)	96.5	92.7	85.6	88.5

Table S2. Electrode voltages of the three-electrode full-cell at different current rates with a voltage range of 1.5-3.2V.

	NMC cathode			TNO@C anode		
Voltage (V)	Discharging limit	Charging limit	Window	Charging limit	Discharging limit	Window
C/10	3.46	4.15	0.69	1.95	0.95	1.00
4C	3.37	4.31	0.94	1.90	1.12	0.78
5C	3.36	4.33	0.97	1.86	1.14	0.72
6C	3.35	4.34	0.99	1.85	1.16	0.69

Table S3. Concentrations of XPS characteristic peaks for NMC and TNO@C electrodes before and after XFC cycling.

Characteristic peaks	Fresh NMC	Cycled NMC	Fresh TNO@C	Cycled TNO@C
C-C, C-H	40.72%	35.22%	47.59%	31.93%
C-OH, C-O-C	18.60%	26.41%	17.97%	19.53%
C=O	15.89%	14.82%	12.49%	23.60%
O-C=O	4.02%	9.69%	5.69%	9.33%
PVDF	20.78%	13.86%	16.25%	15.60%
C=O	56.18%	65.53%	31.79%	48.16%
O-C=O	14.47%	34.47%	9.88%	22.54%
O^{2-}	29.35%	N/A	N/A	N/A
O-H	N/A	N/A	58.33%	29.31%
C-F	100%	78.40%	100%	79.89%
LiF	N/A	21.60%	N/A	20.11%